

Corrosion Testing Of Additively Manufactured Stainless Steel 316H In Molten Salt Environments

SEPTEMBER 2024

Trishelle M. Copeland-Johnson, Michael E. Woods,
Kyle R. Holloway, and Andrea M. Jokisaari

Idaho National Laboratory



DISCLAIMER

This information was prepared as an account of work sponsored by an agency of the U.S. Government. Neither the U.S. Government nor any agency thereof, nor any of their employees, makes any warranty, expressed or implied, or assumes any legal liability or responsibility for the accuracy, completeness, or usefulness, of any information, apparatus, product, or process disclosed, or represents that its use would not infringe privately owned rights. References herein to any specific commercial product, process, or service by trade name, trade mark, manufacturer, or otherwise, does not necessarily constitute or imply its endorsement, recommendation, or favoring by the U.S. Government or any agency thereof. The views and opinions of authors expressed herein do not necessarily state or reflect those of the U.S. Government or any agency thereof.

Corrosion Testing Of Additively Manufactured Stainless Steel 316H In Molten Salt Environments

**Trishelle M. Copeland-Johnson, Michael E. Woods,
Kyle R. Holloway, and Andrea M. Jokisaari
Idaho National Laboratory**

September 2024

**Idaho National Laboratory
Idaho Falls, Idaho 83415**

<http://www.inl.gov>

**Prepared for the
U.S. Department of Energy
Office of Nuclear Energy
Under DOE Idaho Operations Office
Contract DE-AC07-05ID14517**

Page intentionally left blank

ABSTRACT

The development of standard practices for evaluating the corrosion resistance of additive manufactured (AM) stainless steel (SS) 316H in chloride molten salts is critical for the use of these materials in extreme environments such as molten salt reactors (MSRs). This report pertains to a work package of the Advanced Materials and Manufacturing Technologies (AMMT) program developing a systematic methodology linking changes in AM fabrication parameters, namely surface finishing, porosity, microstructure, and chemical heterogeneity, to corrosion performance in NaCl-MgCl₂ salt, a proposed secondary coolant for MSRs. During Fiscal Year 2024, Idaho National Laboratory investigators in the AMMT program utilized SS316H bars fabricated via laser bed powder fusion at Los Alamos National Laboratory (LANL) to establish and optimize the workflow for evaluating these process-to-performance relationships. Standard practices for specimen preparation were established using these specimens, focusing on descaling and sectioning methods that align with ASTM guidelines. A comprehensive experimental design for static corrosion testing was developed, with pre- and post-exposure analysis utilizing optical microscopy and scanning electron microscopy. Standard descaling techniques were optimized, one static corrosion test was conducted on the LANL AM SS316H specimens, establishing pre- and post-corrosion practices. In addition, the work package yielded a review paper on corrosion testing gaps for AM materials in nuclear applications. This work package establishes a foundation for evaluating processing-to-performance relationships for AM SS316H in harsh conditions, contributing to the safe and efficient design of components for next-generation nuclear reactors. The creation of a standardized methodology and the generation of relevant publications and future research pathways represent significant strides towards addressing the crosscutting technology mission of AMMT; these standard practices can be applied to the material for study of corrosion in sodium, fueled salt, and other environments.

Page intentionally left blank

ACKNOWLEDGMENTS

This work was funded by the Advanced Materials and Manufacturing Technologies program, which is supported by the Office of Nuclear Energy of the U.S. Department of Energy. This research was supported at the Idaho National Laboratory, which is supported by the Office of Nuclear Energy of the U.S. Department of Energy and the Nuclear Science User Facilities under Contract No. DE-AC07-05ID14517.

Page intentionally left blank

CONTENTS

| | |
|--|-----|
| ABSTRACT | iii |
| ACKNOWLEDGMENTS | v |
| 1. INTRODUCTION | 1 |
| 2. EXPERIMENTAL DESIGN | 2 |
| 2.1. SAMPLE PREPARATION | 2 |
| 2.1.1. Overview of AM SS 316H specimens procured from LANL..... | 2 |
| 2.1.2. Establishing standard practices for removing surface contaminants with descaling techniques | 5 |
| 2.2. STATIC CORROSION TESTING | 6 |
| 2.2.1. Description of static corrosion testing experimental setup | 6 |
| 2.2.2. Static corrosion testing matrix | 8 |
| 2.2.3. Pre-Corrosion and Post-Corrosion Evaluation..... | 9 |
| 3. PUBLICATIONS AND HARVEST STRATEGIES | 9 |
| 3.1. PEER-REVIEWED PUBLICATIONS | 10 |
| 3.2. HARVEST STRATEGIES | 11 |
| 4. DISCUSSION & CONCLUSIONS | 11 |
| 4.1. Discussion | 11 |
| 4.2. Conclusions | 12 |
| 5. REFERENCES | 13 |
| References | 13 |

FIGURES

| | | |
|-----------|--|----|
| Figure 1. | Schematics illustrating sectioning plans for LPBF LANL SS316H bars. | 4 |
| Figure 2. | Images of Bar #3 before and after acid pickling in HNO_3/HF | 6 |
| Figure 3. | Custom boron nitride sample holder for static corrosion tests. | 8 |
| Figure 4. | Image of the side-of-print surface from a bar #3 specimen produced using LSCM..... | 10 |

TABLES

| | |
|---|---|
| Table 1. Print parameters for LPBF SS 316H bars procured from LANL. | 3 |
| Table 2. ICP-MS results of the composition of the powder and bars #3 and #10 after printing. | 5 |
| Table 3. Experimental matrix for corrosion tests. | 7 |

Page intentionally left blank

ACRONYMS

| | |
|---------------------------------------|--|
| Al | aluminum |
| AM | additively manufactured |
| AMMT | Advanced Materials and Manufacturing Technologies |
| ANL | Argonne National Laboratory |
| ASTM | American Society for Testing and Materials International |
| BN | boron nitride |
| CH₃CH₂OH | ethanol |
| Cr | chromium |
| EBSD | electron backscatter diffraction |
| EDM | electric discharge machining |
| EDS | energy dispersive x-ray spectroscopy |
| Fe | iron |
| FY | fiscal year |
| H₂SO₄ | sulfuric acid |
| HCl | hydrochloric acid |
| HF | hydrofluoric acid |
| HNO₃ | nitric acid |
| HTGR | high temperature gas reactors |
| ICP-MS | inductively coupled plasma mass spectrometry |
| INL | Idaho National Laboratory |
| LANL | Los Alamos National Laboratory |
| LPBF | laser powder bed fusion |

| | |
|-------------|------------------------------------|
| LSCM | laser scanning confocal microscopy |
| MgO | magnesium oxide |
| MSR | molten salt reactors |
| NRC | Nuclear Regulatory Commission |
| NSUF | Nuclear Science User Facilities |
| OM | optical microscopy |
| P | phosphorous |
| SE | standard error of the mean |
| SEM | scanning electron microscopy |
| SFR | sodium cooled fast reactors |
| Si | silicon |
| SS | stainless steel |
| Ta | tantalum |

Page intentionally left blank

Corrosion Testing of Additively Manufactured Stainless Steel 316H in Molten Salt Environments

1. INTRODUCTION

Additive manufacturing of nuclear structural materials provides an opportunity to deploy novel geometries and compositions, which may improve overall performance and reduce costs of constructing advanced nuclear reactor concepts, including molten salt reactors (MSR), sodium cooled fast reactors (SFR), and high temperature gas reactors (HTGR) [1]. The Advanced Materials and Manufacturing Technologies (AMMT) program seeks to develop cross-cutting technologies in support of a broad range of nuclear reactor technologies and help maintain U.S. leadership in materials and manufacturing technologies for nuclear energy applications [2]. The overarching vision of the AMMT program is to accelerate the development, qualification, demonstration, and deployment of advanced materials and manufacturing technologies to enable reliable and economical nuclear energy [2].

The advances in additively manufactured (AM) technologies has created new opportunities and challenges for developing novel structural materials and designs for nuclear applications [1, 3]. Compared with traditionally fabricated materials, AM materials possess different defects, microstructures, and internal stress states. Consequently, the properties and service performance of AM materials may be significantly different from their traditionally fabricated counterparts [3, 4]. To fully realize the advantages of AM technologies in support of advanced nuclear technologies, the unique characteristics of AM materials must be understood and their impacts on the service performance must be evaluated [1]. In addition, standards bodies such as American Society for Testing and Materials International (ASTM) help regulatory bodies, such as the Nuclear Regulatory Commission (NRC), systemically evaluate licensing concerns related to corrosion performance of structural materials. However, no ASTM standard exists specifically for testing the corrosion performance of AM materials [1]. An internal standardized methodology for testing is critical, establishing a

foundation to advocate for a new ASTM standard.

The objective of this work package is to establish a systemic standardized methodology that correlates how changes in the AM fabrication parameters (e.g. surface finishing, porosity, microstructure, and chemical heterogeneities, etc.) of laser powder bed fusion (LPBF) stainless steel (SS) 316H impact the corrosion performance in chloride molten salt with regard to the extent of corrosion, microstructural evolution, and selective diffusion of alloying elements. Ultimately, this work package aims to develop processing-to-performance relationships for strategic design of SS 316H for extreme environments. For fiscal year (FY) 2024 the investigators employed LPBF bars acquired from Los Alamos National Laboratory (LANL) to establish standard practices for processing-to-performance evaluations. Investigators evaluated standard practices for sectioning and descaling as-received versus heat treated specimens in accordance with ASTM guidelines, evaluating specimens before and after cleaning using optical microscopy (OM) and scanning electron microscopy (SEM) techniques. The experimental design for static corrosion testing in NaCl-MgCl₂ salt was also established. The NaCl-MgCl₂ salt system was selected because it is a well-investigated secondary coolant for MSR [5]. The investigators also produced notable information products, including a review paper discussing the technical gap in corrosion testing of AM materials for nuclear reactor applications. The creation of a standardized methodology and the generation of relevant publications and future research pathways represent significant strides towards addressing the crosscutting technology mission of AMMT; these standard practices can be applied to future studies of corrosion in sodium, fueled salt, and other environments.

2. EXPERIMENTAL DESIGN

2.1. SAMPLE PREPARATION

2.1.1. Overview of AM SS 316H specimens procured from LANL

Four bars of SS 316H, labelled #3, #6, #8, and #10, were printed at LANL using LPBF with printing parameters provided in Table 1. Bars #3 and #10 were thermally aged at 650 °C for 94 hours in air, then air-cooled. These specimens developed a substantial oxide layer post thermal aging that would prove beneficial

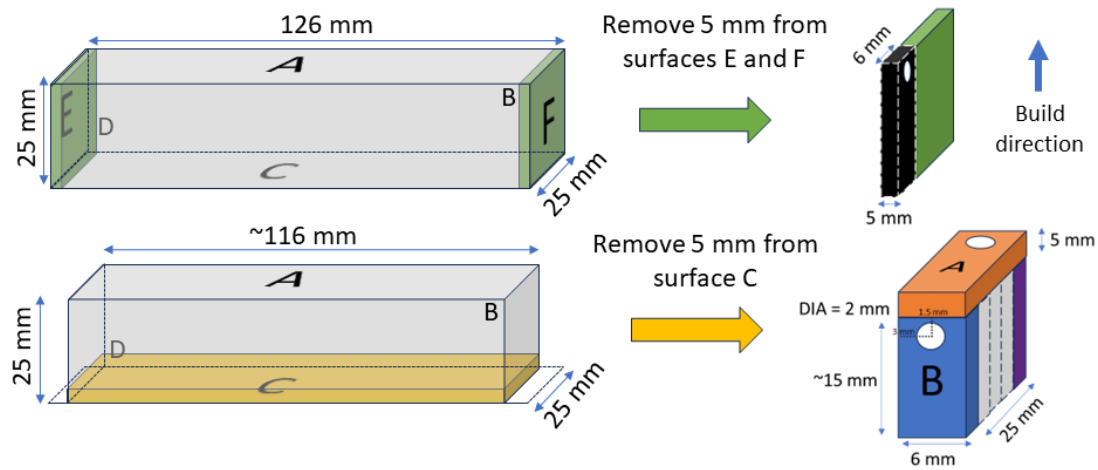
in the development of standard surface cleaning procedures and should also have developed significant carbide precipitates beneficial for assessing carbide behavior on rough printed surfaces. Bars #6 and #8 were sectioned into specimens as-received, providing samples that have not undergone any thermal aging to be used in testing of various post-fabrication heat treatment and with a minimal oxide layer for baseline assessment of cleaning procedures.

Table 1. Print parameters for LPBF SS 316H bars procured from LANL.

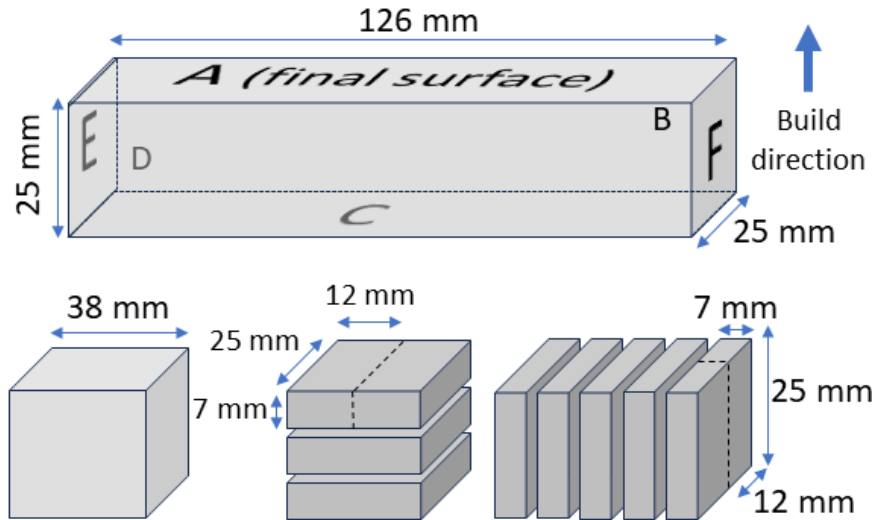
| Parameter | Value |
|---------------------------|----------------------|
| Build direction | Vertical |
| Laser path | Horizontal |
| Laser power | 275 W |
| Speed | 688 mm/s |
| Volumetric Energy Density | 95 J/mm ³ |

Different sectioning plans and techniques were investigated, but unlike corrosion tests on conventional material on machined and polished surfaces, the specimen location within the bar was considered as a test variable. Thus, all sectioning plans specifically involved removing the printed surface layers and retaining them as test specimens, as well as sectioning the interior of the bars. Bars #3 and #10 (thermally aged specimens) were cut by electric discharge machining (EDM) into 80 coupons with similar dimensions in varied locations in order to create unique test specimens with varied surfaces from the printed bar. The sectioning plan is shown in Figure 1a. Concerns about residual copper implantation and localized heating due to EDM, which could unintentionally alter the specimen surface composition and microstructure, prompted updating the sectioning plan to low-speed sectioning for bars #6 and #10 (as-received). Bar #6 was sectioned as-received by a Buehler IsoMet low-speed saw with a diamond wafering blade. In addition, the sectioning plan, shown in Figure 1b, was updated to better accommodate different orientations with respect to the build plate providing different perspectives for studying how corrosion performance is influenced by directional residual stresses from the build process and the effects of heat treatments to relieve these stresses.

The composition of the powder used in the printing process was studied by inductively coupled plasma mass spectrometry (ICP-MS) and provided by LANL. Additionally, samples of bars #3 and #10 were



(a) Sectioning plan for bars #3 and #10 to create test specimens.



(b) Sectioning plan for bar #6 to create test specimens.

Figure 1. Schematics illustrating sectioning plans for LPBF LANL SS316H bars.

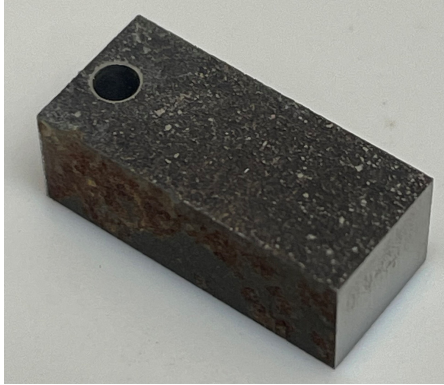
analyzed by ICP-MS at Idaho National Laboratory (INL) with results shown in Table 2; note that standard error of the mean (SE) was within the 95% confidence interval. It was evident that while the input powder feedstock did meet the ASTM specification for SS316H, the printed material did not, with significant loss of iron (Fe) and chromium (Cr) and gains of silicon (Si), aluminum (Al), and phosphorous (P).

Table 2. ICP-MS results of the composition of the powder and bars #3 and #10 after printing.

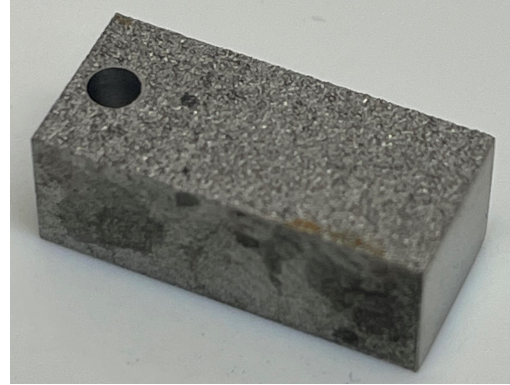
| Element | ASTM Specification (wt%) | Powder (wt%) | Bar #3(wt% \pm SE) | Bar #10(wt% \pm SE) |
|---------|--------------------------|--------------|----------------------|-----------------------|
| Fe | balance | 68.37 | 61.12 \pm 0.90 | 61.39 \pm 2.68 |
| Cr | 16.0-18.0 | 16.94 | 14.83 \pm 0.19 | 14.92 \pm 0.51 |
| Ni | 10.0-14.0 | 10.88 | 10.26 \pm 0.12 | 10.44 \pm 0.39 |
| Mo | 2.00-3.00 | 2.23 | 2.10 \pm 0.03 | 2.09 \pm 0.08 |
| Mn | <2.00 | 1.02 | 0.83 \pm 0.01 | 0.83 \pm 0.03 |
| Si | <1.00 | 0.37 | 3.35 \pm 0.25 | 3.26 \pm 0.06 |
| Al | n/a | 0.01 | 0.24 \pm 0.01 | 0.24 \pm 0.00 |
| P | <0.045 | 0.03 | 0.38 \pm 0.02 | 0.38 \pm 0.00 |
| C | <0.04-0.10 | 0.043 | n/a | n/a |

2.1.2. Establishing standard practices for removing surface contaminants with descaling techniques

Following the assessments and recommendations from Ref. [1], one objective within this FY-24 work was the establishment of best practices for handling and preparation of AM specimens for corrosion testing. Unlike conventionally manufactured components, which are deployed with a machined surface, AM components may be deployed with an as-manufactured surface roughness, either to reduce cost or because the geometry cannot be machined (e.g., interior channels). In addition, the microstructure and residual stresses in AM components may be significantly anisotropic and vary across the build, meaning that specimens must be linked to their location and orientation within the original build geometry. Thus, this project consulted established standard procedures applied to conventionally wrought counterparts in commercial settings, including procedures for removing surface contaminants (e.g., oxides, grease, oil) from the surface prior to using thorough descaling techniques. Standard acid descaling procedures of wrought SS316 materials are provided in Table A1.1 of the ASTM standard ASTM A380/A380M-17 [6]. From this standard, a mix of 8% nitric acid (HNO_3) and 1.5% hydrofluoric acid (HF) was chosen. A second acid mixture, consisting of 15% sulfuric acid (H_2SO_4), 7% hydrochloric acid (HCl), and 7% HNO_3 was also tested based upon the procedure established by members of the AMMT Argonne National Laboratory (ANL) team. Specimens of the heavily oxidized bar #3 were pickled using the HNO_3 /HF mixture at 60°C for periods of 5 minutes and pickled using the H_2SO_4 /HCl/ HNO_3 mixture at 80°C for periods of 3 minutes. After each period of immersion in the acid mixtures, the specimens



(a) Bar #3 specimen before acid pickling.



(b) Bar #3 specimen after acid pickling.

Figure 2. Images of Bar #3 before and after acid pickling in HNO_3/HF .

were cleaned of residual acid via immersion in two, deionized water baths. Mechanical brushing was then performed with a brass brush, and subsequent rounds of acid immersion, rinsing in deionized water, and drying with forced air were performed until the sample appeared visually clean and exhibited a familiar "white pickled finish".

The specimens from bar #3 showed clean surfaces after three rounds of pickling and mechanical brushing for each acid mixture case, as shown in Figures 2a and 2b. The discoloration on the foreground edge of the specimen after cleaning suggested that the rinsing and drying procedure employed were not adequate to properly clean the sample of residual acid and water. The final recommended procedure for cleaning and drying specimens following acid exposure was employed for later acid pickled samples, and consists of sonication in deionized water, followed by sonication in ethanol ($\text{CH}_3\text{CH}_2\text{OH}$), and an additional rinse with $\text{CH}_3\text{CH}_2\text{OH}$, and final drying with forced air.

2.2. STATIC CORROSION TESTING

2.2.1. Description of static corrosion testing experimental setup

Static corrosion testing was utilized as a preliminary approach for assessment of corrosion performance. Future investigations could prioritize studying materials in a configuration closer to their operating environment, namely in a flow corrosion loop. Salt corrosivity is enhanced by impurities including water,

oxygen, fission products (e.g. tellurium, uranium, etc.) and dissolved alloying elements [5]. Therefore, it was imperative that any corrosion testing in molten salts included a well-designed purification process and be conducted under highly controlled atmosphere.

Static corrosion tests were conducted within an argon atmosphere glovebox maintained at < 1 ppm oxygen and < 1 ppm water atmosphere. The salts were held within alumina crucibles with a submerged boron nitride sample holder to orient the samples and allow for removal from the salt while still hot. The design of the boron nitride (BN) holder for these samples is shown in Figure 3. All components were cleaned outside the glovebox using deionized water and $\text{CH}_3\text{CH}_2\text{OH}$, followed by air drying and vacuum oven drying at 120°C for 1 hour. The alumina crucibles were also pre-cleaned using a 2% nitric acid solution and then were baked at 800°C within the glovebox. Salt preparation procedure was inspired by published practices from Oak Ridge National Laboratory [7]. The process began with NaCl-MgCl₂ eutectic salt (56.3 mol% NaCl) prepared from commercial high-purity anhydrous NaCl and MgCl₂ by mixing the appropriate amounts within a glassy carbon crucible and drying the salts within a vacuum oven for 2 hours successively at 120, 180, 240, and 300°C to drive off hydration and avoid the formation of magnesium oxide (MgO) and hydroxides through hydrolysis at higher temperatures. The salts were then heated to 600°C within the glovebox furnace. After two hours at this temperature, 5 wt% Mg metal was added to react any oxygen present forming MgO precipitates that settled at the bottom of the crucible. The purified molten salts were then carefully decanted onto a nickel dish, avoiding agitating the contents so that the MgO precipitates remained at the bottom of the crucible, and were allowed to cool and solidify before use in corrosion tests.

Table 3. Experimental matrix for corrosion tests.

| Sample | Pickling | Exposure | Polished Sides | Pre-Corrosion OM | Post-Corrosion OM |
|--------|----------------------|------------------------|----------------|------------------|-------------------|
| 1a | None | Thermal Only | No | Yes | Yes |
| 1b | None | Thermal Only | No | No | No |
| 2a | None | NaCl-MgCl ₂ | No | Yes | Yes |
| 2b | None | NaCl-MgCl ₂ | No | No | No |
| 3a | HNO ₃ /HF | NaCl-MgCl ₂ | No | Yes | Yes |
| 3b | HNO ₃ /HF | NaCl-MgCl ₂ | No | No | No |
| 4 | None | None | Yes | Yes | Yes |

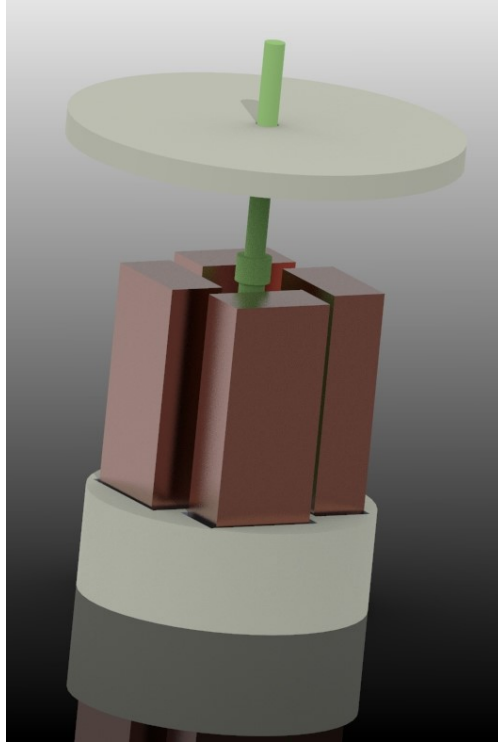


Figure 3. Custom boron nitride sample holder for static corrosion tests.

2.2.2. Static corrosion testing matrix

For FY-24, one static corrosion test set was conducted on internally sectioned specimens from bar # 6, parallel to the build direction, Figure 1b. The goal of this test was to compare the evolution in the morphology of the fabricated surfaces and microstructure between two experimental conditions: 1) thermal aging only versus corrosion + thermal aging, deconvoluting the role of temperature from the corrosion attack, and 2) pickling versus no pickling, comparing the impact of the identified pickling procedure on experimental results. An illustration of the test matrix is featured in Table 3. Thermal control, also referred to as thermal only specimens, were only subjected to thermal aging while in the same furnace as the corroded specimens. Specimens marked for corrosion were housed within the aforementioned alumina crucibles, set in the custom-designed BN well plates, illustrated in Figure 3.

One as-received specimen was included as a baseline, with all slow-speed cut sides mechanically polished down to $0.25\mu\text{m}$ with a diamond slurry as a point of comparison to the AM printed surfaces during

pre-corrosion evaluation with laser scanning confocal microscopy (LSCM). Additionally, duplicate thermal control specimens were included in the test matrix, sealed within a quartz ampoule to atmospherically isolate the specimen from the furnace. The ends of the thermal control were electrically isolated from making contact with the ampoule walls by BN end pieces. An additional protection of atmospheric isolation was provided in the form of a tantalum (Ta) foil strip within the ampoule. Both the as-received and thermal control specimens were not subjected to the standard cleaning procedure. Four specimens were corroded in the NaCl-MgCl₂ eutectic salt mixture, one as-received and one that underwent the acid descaling.

2.2.3. Pre-Corrosion and Post-Corrosion Evaluation

A select group of specimens, each representing an experimental variable, were or will be characterized before and after corrosion using LSCM and SEM techniques. LSCM is an optical microscopy technique utilizing a high resolution laser to scan and quantify topographical changes in surface morphology. The evolution of the fabrication surfaces was quantified, contextualizing where on the specimen the most material was lost. This information pinpointed vulnerable regions of the fabricated surface that were most susceptible to attack and will then be correlated to SEM analysis. Figure 4 is an example of the quantitative LSCM results from a specimen originating from bar #3 prior to corrosion. Evident on the surface was residual unmelted powder (spherical particles) in addition to larger irregular particles, potentially slag. SEM analysis will then focus on compositional heterogeneities in localized regions of enhanced corrosion identified during LSCM and the evolution of bulk composition using SEM energy dispersive x-ray spectroscopy (EDS) and bulk microstructure using electron backscatter diffraction (EBSD).

3. PUBLICATIONS AND HARVEST STRATEGIES

The investigators of this manuscript are pleased to report that they have generated a peer-reviewed publication and are exploring harvest strategies into efforts beyond the original scope of the work package

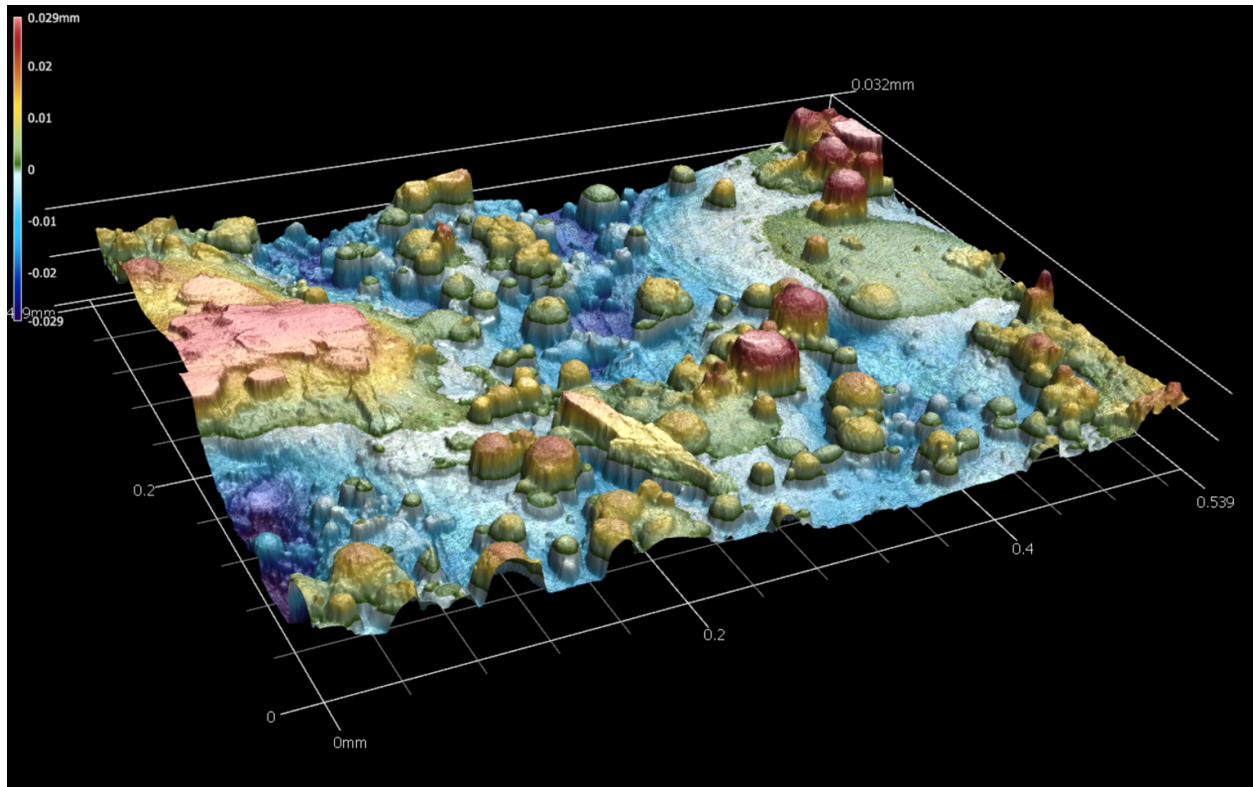


Figure 4. Image of the side-of-print surface from a bar #3 specimen produced using LSCM.

that will be beneficial to the AMMT program.

3.1. PEER-REVIEWED PUBLICATIONS

A manuscript titled "Corrosion testing needs and considerations for AM materials in nuclear reactors" was published in Progress in Nuclear Energy, an international review journal covering topics related to nuclear science & engineering. The review article was a multi-institutional effort between members of the AMMT team, led by investigator Jokisaari on the INL team. The paper summarizes advanced nuclear reactor concepts, with emphasis placed on novel challenges of corrosion mitigation and developing a system framework for assessment of AM nuclear structural materials to aid in the development of regulatory bodies and standards around the use of AM materials.

3.2. HARVEST STRATEGIES

Members of the INL team also pursued a rapid turnaround experiment user proposal through the Nuclear Science User Facilities (NSUF) program. The pending proposal, titled "Irradiation and corrosion of additively manufactured 316H stainless steel in molten chloride salt", is led by investigator Woods and proposes conducting ex-situ experiments to elucidate the synergistic effects of ion irradiation and corrosion in molten salts on conventionally wrought and AM SS316H. The proposal includes Dr. Stephen Raiman at the University of Michigan as a collaborator conducting the corrosion work, with ion irradiation studies being conducted at the Michigan Beam Ion Laboratory and post-irradiation examination studies performed at the Electron Microscopy Laboratory at INL.

4. DISCUSSION & CONCLUSIONS

4.1. Discussion

This work package aimed to elucidate the impact of LPBF processing parameters on SS 316H specimens procured from LANL, focusing on establishing standard practices for surface treatment and evaluating corrosion resistance. The specimens underwent various post-fabrication cleaning, and were sectioned to provide a diverse array of surfaces for testing. One significant finding was the deviation of the printed SS316H's elemental composition from the ASTM specifications, despite the powder feedstock meeting the requirements. The loss of Fe and Cr and the gains of Si, Al, and P are noteworthy and may have implications for the material's performance, particularly its corrosion resistance. The establishment of best practices for specimen preparation, such as acid pickling and mechanical brushing, was successful in achieving a "white pickled finish," suggesting the removal of substantial surface contaminants. The effectiveness of this cleaning procedure is crucial as AM components will be deployed under standard commercial standards with an inherent surface roughness from the manufacturing process, which could affect their corrosion resistance. A static corrosion test within a controlled environment was conducted to provide insights into the corrosion

performance of AM SS316H. The test matrix was carefully designed to distinguish the effects of thermal aging from those of corrosion and to evaluate the impact of the pickling procedure on corrosion resistance. The use of advanced microscopy techniques, LSCM and SEM, will then allow for a detailed assessment of surface and microstructural changes pre- and post-corrosion. This analysis will reveal the most vulnerable regions on the fabricated surfaces, guiding future improvements in AM processes and post-treatment procedures.

4.2. Conclusions

In conclusion, the composition of LPBF SS316H derived from LANL deviates from ASTM specifications after the printing process, with a notable loss of Fe and Cr and an increase in Si, Al, and P. This could affect the material's suitability for certain applications, including its corrosion resistance in challenging environments such as nuclear reactors. The developed descaling procedures were effective in cleaning heavily oxidized surfaces. The recommended cleaning and drying procedures from post-acid exposure were critical for preparing AM specimens for corrosion testing and ensuring the reliability of the results. The study's findings contribute to the body of knowledge required to establish industry-wide standards and best practices for the use of AM materials, particularly in the context of nuclear applications. Additionally, the research outcomes have resulted in a peer-reviewed publication and set the stage for further exploration into the combined effects of irradiation and corrosion on AM materials. In FY 2025, research into the effect of process variability on the molten chloride corrosion behavior of rough and machined surfaces of LPBF 316H will continue. A natural outcome of this effort will be the continued development of standard practices that will aid in the assessment of AM materials in nuclear reactors.

5. REFERENCES

- [1] A. M. Jokisaari, Y. Chen, T. Copeland-Johnson, T. Hartmann, V. Joshi, I. van Rooyen, R. Song, and J. Wierschke, “Corrosion testing needs and considerations for additively manufactured materials in nuclear reactors,” *Progress in Nuclear Energy*, vol. 174, p. 105296, 9 2024.
- [2] M. Li, D. Andersson, R. Dehoff, A. Jokisaari, I. van Rooyen, and D. Cairns-Gallimore, “Advanced materials and manufacturing technologies (AMMT) 2022 roadmap,” 2022.
- [3] J. Simpson, J. Haley, C. Cramer, O. Shafer, A. Elliott, W. Peter, L. Love, and R. Dehoff, “Considerations for application of additive manufacturing to nuclear reactor core components,” 2019.
- [4] C. Sun, Y. Wang, M. D. McMurtrey, N. D. Jerred, F. Liou, and J. Li, “Additive manufacturing for energy: A review,” *Applied Energy*, vol. 282, 1 2021.
- [5] S. Guo, J. Zhang, W. Wu, and W. Zhou, “Corrosion in the molten fluoride and chloride salts and materials development for nuclear applications,” *Progress in Materials Science*, vol. 97, pp. 448–487, 8 2018.
- [6] “A380/a380m – 17 standard practice for cleaning, descaling, and passivation of stainless steel parts, equipment, and systems,” 2017.
- [7] K. Robb, S. Baird, J. Massengale, N. Hoyt, J. Guo, and C. Moore, “Engineering-scale batch purification of ternary mgcl₂-kcl-nacl salt using thermal and magnesium contact treatment,” 8 2022.